ORIGINAL ARTICLE

Clinicopathological and molecular analyses of hyperplastic lesions including microvesicular variant and goblet cell rich variant hyperplastic polyps and hyperplastic nodules—Hyperplastic nodule is an independent histological entity

Noriyuki Uesugi[1] | Yoichi Ajioka[2] | Tomio Arai[3] | Yoshihito Tanaka[1] | Tamotsu Sugai[1] (ORCID)

[1]Department of Molecular Diagnostic Pathology, School of Medicine, Iwate Medical University, Shiwagun'yahabachou, Japan

[2]Division of Molecular and Diagnostic Pathology, Graduate School of Medical and Dental Sciences, Niigata University, Niigata, Japan

[3]Department of Diagnostic Pathology, Tokyo Metropolitan Geriatric Hospital and Institute of Gerontology, Tokyo, Itabashiku, Japan

Correspondence

Tamotsu Sugai, Department of Molecular Diagnostic Pathology, Iwate Medical University, 2-1-1, Shiwagun'yahabachou 028-3695, Japan.
Email: tsugai@iwate-med.ac.jp

Abstract

Hyperplastic nodules (HNs) have been considered to be hyperplastic lesions among Japanese pathologists, although they have not been recognized worldwide. Here, we examined clinicopathological and molecular differences between goblet cell-rich variant hyperplastic polyp (GCHPs), microvesicular variant HPs (MVHPs), and HNs. Patients with hyperplastic lesions including 61 GCHPs, 62 MVHPs, and 19 HNs were enrolled in the present study. The clinicopathological and molecular features examined included the mucin phenotype expression, p53 overexpression, annexin A10, genetic mutations (*BRAF* and *KRAS*), and DNA methylation status (low, intermediate, and high methylation epigenotype). In addition, hierarchical cluster analysis was also performed to identify patterns among the histological features. The lesions were stratified into three subgroups and each lesion was assigned into a subgroup. While GCHP was associated with *KRAS* mutation, MVHP was closely associated with *BRAF* mutation; no mutation was found in HN. We list specific histological findings that corresponded to each lesion. Finally, there were no significant differences in the methylation status among lesions. The current result shows that both MVHPs and GCHPs have a neoplastic nature whereas HN is nonneoplastic. We suggest that HNs should be distinguished from HPs, in particular GCHPs, in terms of pathological and genetic features.

KEYWORDS

goblet cell-rich variant, hyperplastic nodule, hyperplastic polyp, *KRAS* mutation

INTRODUCTION

Serrated lesions are generally classified into hyperplastic polyps (HPs), traditional serrated adenomas, and sessile serrated lesions.[1–3] HPs are currently sub-classified into microvesicular variants (MVHPs) and goblet cell-rich variants (GCHPs).[1–3] MVHPs and GCHPs differ in terms of histological features and molecular findings.[1–3] MVHPs are characterized by admixed goblet and columnar cells with microvesicular mucin, inconspicuous

nuclei, and luminal serrations, whereas GCHPs are less serrated and show prominent goblet cells.[1,2] Moreover, while *BRAF* mutation characterizes MVHPs, *KRAS* mutation is frequently found in GCHPs.[1–3] However, DNA methylation may play a role in the development of both lesions.[4–6] These findings suggest that although MVHPs and GCHPs are both neoplastic lesions, they have different natures[1,2] and are independent lesions, both pathologically and clinically.

Apart from these HPs, another hyperplastic lesion characterized by elongated crypts without serration and abundance of goblet cells has been designated as hyperplastic nodule (HN) among Japanese but not Western pathologists.[7] Differential diagnosis of HN from GCHP is difficult due to their similar histology (e.g., elongated crypts with little or no serration, abundance of goblet cells).[7] The histological and molecular characteristics of GCHPs are well recognized, but those of HN have not been investigated. In the present study, we identified clinicopathological and molecular findings of HNs. In addition, we examined the difference in histological and molecular features between MVHPs, GCHPs, and HNs to define the pathological hallmarks of HN.

MATERIALS AND METHODS

Patients

Patients with hyperplastic lesions including 61 GCHPs, 62 MVHPs, and 19 HNs were examined and the clinicopathological findings are shown in Table 1. The histopathological diagnoses of GCHP and MVHP were reached according to the 2019 WHO classification (World Health Organization).[2] In brief, MVHPs were histologically characterized by (1) a "sawtooth" appearance of the upper portion of polyp, (2) small regular round nuclei located basally in the luminal half of crypt, (3) elongated, narrow, and hyperchromatic nuclei at the base of the crypt, (4)

microvesicular cytoplasm, and (5) a variable but low number of goblet cells.[2] GCHPs were histologically characterized by (1) elongated and flat crypts, (2) little serration, (3) goblet cell abundance extending to the surface, and (4) surface tufting.[2] Finally, HNs were histologically defined as lesions accompanied by goblet cell abundance and elongated crypts without serration, in accordance with the Japanese criteria.[7]

To avoid inter-observer variation of histological diagnosis, we discussed differences regarding histological assessment. Agreement could be obtained among four gastrointestinal pathologists (N. U., Y. A., T. A., and T. S.).

Histological features examined in GCHPs, MVHPs, and HNs

To histologically characterize each lesion, we selected nine histological features found among the 142 hyperplastic lesions. As listed in Table S1 and illustrated in Figure S1 these were: (1) goblet cell abundance; (2) limited serrated change, only at the surface of the crypt; (3) serration of the crypt within the upper half of the crypt; (4) branching of the crypt; (5) dilatation of the crypt; (6) lateral spread of the crypt base (e.g., boot-shaped or anchor-shaped crypts); (7) asymmetrical branching; (8) narrowing of the lower crypt; and (9) elongated straightforward crypt without serration.[2,8–12] The first eight factors were defined as a lesion with at least greater than one factors. A finding of "elongated straightforward crypt without serration" was termed as a lesion with more than 50% present within the same tumor. The histological features are illustrated in Figure S1.

To evaluate absorptive epithelial cells within the glands of each lesion, we selected single glands with vertical axes that could be observed from the crypt base to the surface of the crypt. According to this method, we counted the number of absorptive epithelial cells and goblet cells in the single glands selected in each lesion.

TABLE 1 Clinicopathlogical features of colorectal hyperplastic lesions

		GCHP (%)	HN (%)	MVHP (%)	*p*-value
Total		61	19	62	
Man:Woman		49:12	13:6	48:14	0.5552
Age (years old)	Range (mean)	29–84 (61)	35–77 (74)	31–79 (61)	N. S.
Locus	Right	13 (21.3)	5 (21.7)	23 (37.1)	0.1495
	Left	48 (78.7)	14 (78.3)	39 (62.9)	
Size (mm)	Range (mean)	2–20 (6)	1–10 (6)	3–13 (7)	N. S.
Macroscopical type	Protruded type	32 (52.5)[*,#]	17 (89.5)[*]	45 (72.6)[#]	0.0044
	Flat elevated type	29 (47.5)[*,#]	2 (10.5)[*]	17 (27.4)[#]	

Abbreviations: GCHP, goblet cell-rich hyperplastic polyp; HN, hyperplastic nodule; MVHP, microvesicular hyperplastic polyp; N. S., not significant.
[*]*p* < 0.05;
[#]*p* < 0.05.

We measured the ratio of absorptive epithelial cells among the total cell population (absorptive epithelial cells and goblet cells). The ratio of absorptive epithelial cells was significantly higher in MVHPs than in HNs and GCHPs ($p < 0.001$; Figure S2).

Immunohistochemistry

Immunostaining was carried out on 3-μm-thick paraffin sections. After deparaffinization and rehydration, the sections were heated in Envision FLEX target retrieval solution (pH 6.0 or 9.0; Dako) for 20 min and washed 2×5 min in phosphate-buffered saline. Endogenous peroxidase was blocked with 3% hydrogen peroxide for 5 min. Non-specific binding was blocked with 1.5% normal serum in phosphate-buffered saline for 35 min at room temperature. Immunohistochemical staining was performed as described previously. Immunohistochemical analysis used anti-p53 (DO7; Dako), anti-MUC2 (Ccp58; Novocastra), anti-MUC5AC (CLH2; Novocastra), anti-MUC6 (CLH5; Novocastra), anti-CD10 (56C6; Novocastra), Annexin A10 (polyclonal; Novusbio), and anti-Ki67 (MIB1, monoclonal; DAKO). Detailed data are presented in Table S2.

Assessment of immunohistochemical expression

To avoid being arbitrary, we used the following criteria to analyze staining of mucin markers (MIUC2, MUC5AC, and MUC6), CD10, p53, and annexin A10. Staining intensity scores were divided into no staining, weak or equivocal staining, moderate staining, and strong staining. Both moderate and strong staining were considered positive expression. The scoring of cells with positive expression was: 0 for 0%–10% of cells; 1 for 10% to <30% of cells; 2 for 30% to <60% of cells; 3 for 60% to <100% of cells; and 4 for 100% of cells. In this study, a score >1 was classified as positive expression of the markers, according to previous study.[13]

To evaluate the Ki67-positive index, two representative adjacent crypts running from the bottom to the surface of the crypt were selected in each specimen. The percentage of Ki67-expressing cells per crypt was separately calculated for the upper, middle, and lower parts of crypt.[14] Depending on the result, each case was classified as upper, middle, and lower.

DNA extraction

Tissue for DNA extraction was micro-dissected from the central area of the lesions. DNA was extracted from isolated normal and tumor tissue by sodium dodecyl sulfate lysis and proteinase K digestion, followed by a phenol-chloroform procedure.

Analysis of KRAS and BRAF mutation

Mutations of *KRAS* and *BRAF* genes were examined using a pyrosequencer (Pyromark Q24; Qiagen NV) and primers as previously described.[15]

Pyrosequencing for evaluation of methylation

We used a two-panel method to determine genome-wide methylation status as in a previous report.[16,17] The DNA methylation status of each gene promoter region was established by PCR analysis of bisulfite-modified genomic DNA (EpiTect Bisulfite Kit; Qiagen) using pyrosequencing for quantitative methylation analysis (Pyromark Q24; Qiagen). In brief, six markers (*RUNX3*, *MINT31*, *LOX, NEUROG1*, *ELMO1*, and *THBD*) were selected for determination of genome-wide methylation status. After methylation analysis of a panel of three markers (*RUNX3*, *MINT31*, and *LOX*), tumors with high (hypermethylated) methylated epigenomes (HMEs) were defined as those with at least two methylated markers. The remaining tumors were examined using three additional markers (*NEUROG1*, *ELMO1*, and *THBD*). Tumors were designated as having intermediately methylated epigenomes (IMEs) if they had at least two methylated markers. Tumors that were not HMEs or IMEs were designated as having low (hypomethylated) methylated epigenomes (LMEs). The cut-off value for the mutation assay was 15% mutant alleles, while that for the methylation assay was 30% of tumor cells, as previously reported.[15]

Hierarchical analysis of the expression of histological features

Hierarchical cluster analysis was performed for clustering of the samples according to the histological findings in order to achieve maximal homogeneity for each group, and the greatest difference between the groups, using open-access clustering software (Cluster 3.0 software; bonsai.hgc.jp/~mdehoon/software/cluster/software.htm). The clustering algorithm was set to centroid linkage clustering, which is standard for biological studies.

Statistical analysis

Data obtained for clinicopathological findings, histological features, immunohistochemical markers, mutations (*KRAS* and *BRAF*), and methylation status based on each lesion were analyzed using χ^2 tests with the aid of Stat Mate-III software (Atom). If statistical differences between the three lesions were found, statistical analysis between two groups was further performed using χ^2 tests

(Stat Mate-III software). Differences in age distributions between the three lesions were evaluated using Kruskal–Wallis H tests with the aid of Stat Mate-III software (Atom). If statistical differences between the three lesions were observed, statistical differences were further evaluated using the same method. Differences with p values of less than 0.05 were considered significant.

RESULTS

Representative histological and immunohistochemical figures of MVHP, GCHP, and HN lesions are shown in Figure 1.

Clinicopathological characteristics among GCHP, MVHP, and HN lesions

We compared clinicopathological characteristics with each hyperplastic lesion (Table 1). The frequency of the macroscopic flat elevated type was significantly higher in GCHP than in MVHP and HN cases ($p < 0.05$;

Table 1). There were no significant differences in the frequency of the other clinicopathological variables (sex, age, tumor location, and tumor size) between lesions.

Association of histological features with each lesion

We investigated the association of the nine histological features with GCHP, MVHP, and HN (Table 2). There was a significant difference in the frequency of eight of the features between the three lesions, but not "lateral spread of the crypt base." In addition, these eight features showed significant differences between each pair of lesions (GCHP vs. MCHP; GCHP vs. HN; MSHC vs. HN). First, we found a significant difference between GCHP and MVHP in the frequency of three features: "goblet cell abundance," "serration of the crypt within the upper half of the crypt," and "branching of the crypt." Second, although the frequency of two features ("limited serrated change, only at the surface of the crypt" and "serration of the crypt with the upper half of
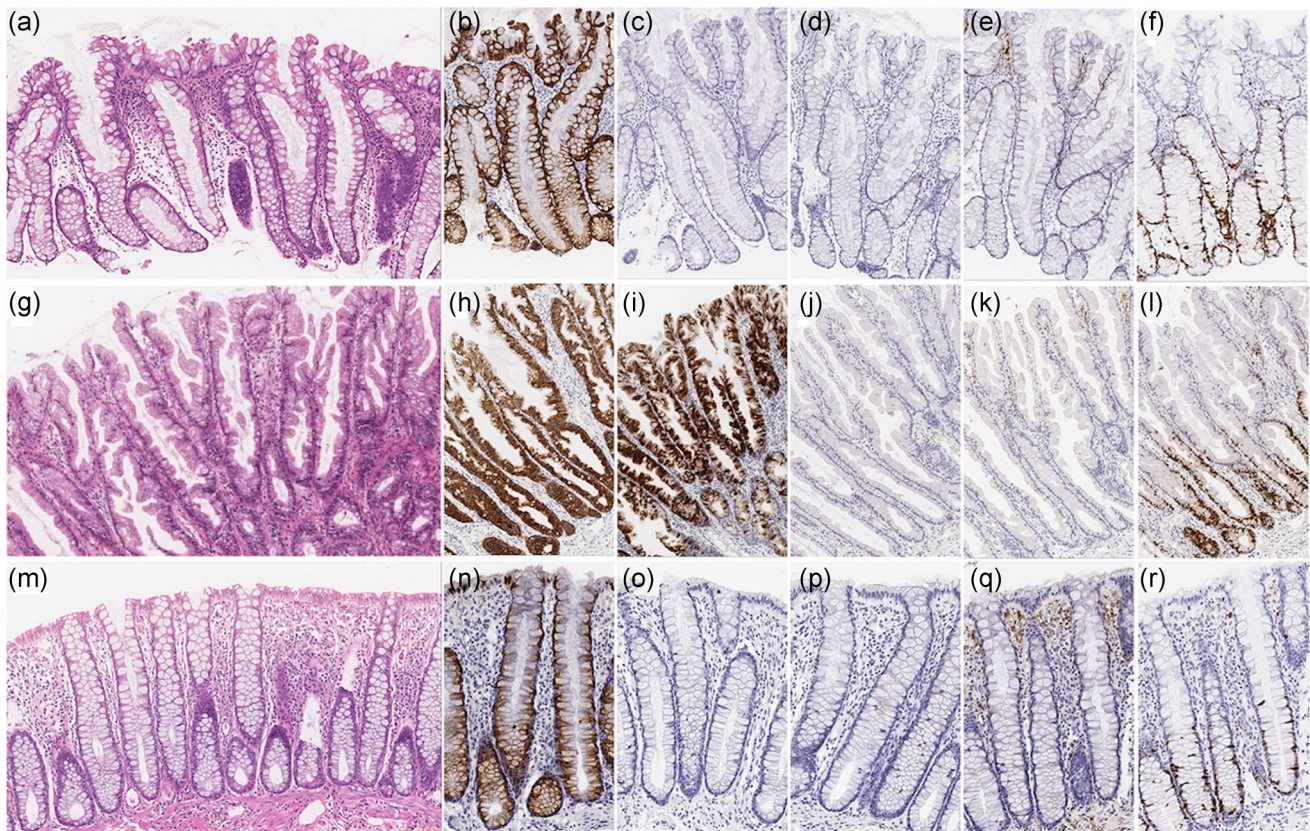

FIGURE 1 Representative figure of hyperplastic lesions: (a) GCHP, (g) MVHP, and (m) HN. (a–f) Goblet cell-rich variant hyperplastic polyp (GCHP); (a) HE staining, (b) MUC2, (c) MUC5AC, (d) MUC6, (e) CD10, (f) Ki-67; (g–l) microvesicular variant hyperplastic polyp (MVHP); (g) HE staining, (h) MUC2, (i) MUC5AC, (j) MUC6, (k) CD10, (l) Ki-67; (m–r) hyperplastic nodule (HN); (m) HE staining. (n) MUC2, (o) MUC5AC, (p) MUC6, (q) CD10, (r) Ki-67. GCHP, goblet cell-rich hyperplastic polyp; HE, hematoxylin and eosin; HN, hyperplastic nodule; MVHP, microvesicular hyperplastic polyp

the crypt") were significantly higher in GCHP than in HN, the frequency of "elongated straightforward serrated crypt without serration" was statistically lower in GCHP than in HN. Third, there was a significant difference in the frequency of "goblet cell abundance" and "elongated straightforward crypt without serration" between HN and MVHP, with HN > MCHP, while the statistical difference in the frequency of "serration of the crypt within the upper half of the crypt," "dilatation of the crypt," and "narrowing of the lower crypt" between HN and MVHP had HN < MVHP. Finally, although HN consisted of an admixture of goblet cell-rich and absorptive cells, GCHP was predominantly composed of goblet cells. In summary, two features were closely associated with GCHPs: "goblet cell abundance" and "limited serrated change within the superficial area of the crypt." Four features characterized MVHPs: "serration of the crypt with the upper half of the crypt," "branching of the crypt," and "dilatation of the crypt and narrowing of the lower crypt." Finally, "elongated straightforward serrated crypt without serration" was the distinctive feature of HNs. Detailed findings are summarized in Table 2.

Differences in immunohistochemical marker expression, gene mutations (*KRAS* and *BRAF*), and DNA methylation status among lesions

Although the frequency of MUC5AC was significantly lower in HNs (0/19) than in GCHPs (0/61) and MVHPs (53/62, 85.5%); $p < 0.001$, the frequency of MUC6 was significantly higher in MVHPs (5/62, 8.1%) than GCHPs

(0/61) and HNs (0/19; $p = 0.0274$; Table 3). To investigate whether morphological changes in hyperplastic lesions were associated with cell proliferation, we performed immunohistochemical examination for Ki67. In HNs, Ki67-positive cells were predominantly found in the lower third of the crypt. In MVHPs, although Ki67-positive cells were primarily observed in the middle third of the crypt, Ki67-positive cells were broadly expanded toward the middle part of the crypt in GCHPs in comparison with HNs and MVHPs. In addition, a low frequency of Annexin A10 expression was common among the lesions. The frequency of *KRAS* mutations was significantly higher in GCHPs than in MVHPs and HN. By contrast, there was a significant difference in the frequency of *BRAF* mutations between GCHPs and HNs and between GCHPs and MVHPs (MVHPs > GCHPs and HNs). Detailed mutation data for *KRAS* and *BRAF* are summarized in Table S2. No differences in the codon of *KRAS* mutations were observed among the three lesion types. In addition, the *KRAS* mutation type did not differ among the lesion types. Finally, no significant differences in methylation status were observed among lesions. The detailed findings are presented in Table 3.

Hierarchical cluster analysis using the nine histological features

We examined the patterns of nine histological features using heat-map hierarchical cluster analysis to identify associations of the histological features with each lesion. Three distinct subgroups were stratified based on the histological features (Figure 2). In clinicopathological

TABLE 2 Differences of histological findings in colorectal hyperplastic lesions

	GCHP (%)	HN (%)	MVHP (%)	*p*-value
Total	61	19	62	
Goblet cell abundance	61 (100)*	19 (100)#	0*,#	3.78E−42
Limited serrated change at superficial area of the crypt	33 (54.1)*,#	0*	0#	1.91E−16
Serration of the crypt with the upper half of the crypt	25 (41.0)*,♭	0*,#	62 (100)#,♭	1.73E−23
Branching of the crypt	18 (29.5)**	5 (26.3)	33 (53.2)**	0.0121
Dilatation of the crypt	16 (26.2)**	2 (10.5)#	31 (50.0)**,#	0.0013
Lateral spread of the crypt base (such as boot- shaped or anchor-shaped crypts)	0	0	0	N. S.
Asymmetrical branching	0	0	6 (9.7)	0.0116
Narrowing of lower crypt	0*	0#	36 (58.1)*,#	7.03E−17
Elongated straightforward crypt without serration	5 (8.2)*	19 (100)*,#	0#	1.90E−20

Abbreviations: GCHP, goblet cell-rich hyperplastic polyp; HN, hyperplastic nodule; MVHP, microvesicular hyperplastic polyp; N. S., not significant.
*$p < 0.01$;
#$p < 0.01$;
♭$p < 0.01$;
**$p < 0.05$.

TABLE 3 Differences of molecular findings in colorectal hyperplastic lesions

		GCHP (%)	HN (%)	MVHP (%)	*p*-value
Total		61	19	62	
MUC2		61 (100)	19 (100)	62 (100)	N. S.
MUC5AC		0*	0#	53 (85.5)*,#	1.068E−29
MUC6		0	0	5 (8.1)	0.0274
CD10		0	0	0	N. S.
Ki-67 distribution	Lower type	27 (44.3)*,#	19 (100)*,**	5 (8.1)#,**	2.39E−09
	Middle type	34 (55.7)*,#	0*,**	56 (90.3)#,**	
	Upper type	0	0	1 (1.6)	
p53		0	0	0	N. S.
Annexin A10		0	0	6 (9.7)	0.0116
KRAS mutation		30 (49.2)*,#	0*	13 (21.0)#	3.18E−06
BRAF mutation		0*	1 (4.3)#	38 (61.3)*,#	6.99E−17
No mutation		31 (50.8)*	18 (96.7)*,#	11 (17.7)#	6.75E−10
DNA methylation	LME	37 (82.2)	12 (75.0)	40 (64.5)	0.3194
	IME	7 (15.6)	4 (25.0)	19 (30.6)	
	HME	1 (2.2)	0	3 (4.2)	

Abbreviations: GCHP, goblet cell-rich hyperplastic polyp; HN, hyperplastic nodule; HME, high-methylation epigenotype; IME, intermediate-methylation epigenotype; MVHP, microvesicular hyperplastic polyp; LME, low-methylation epigenotype; N. S., not significant.
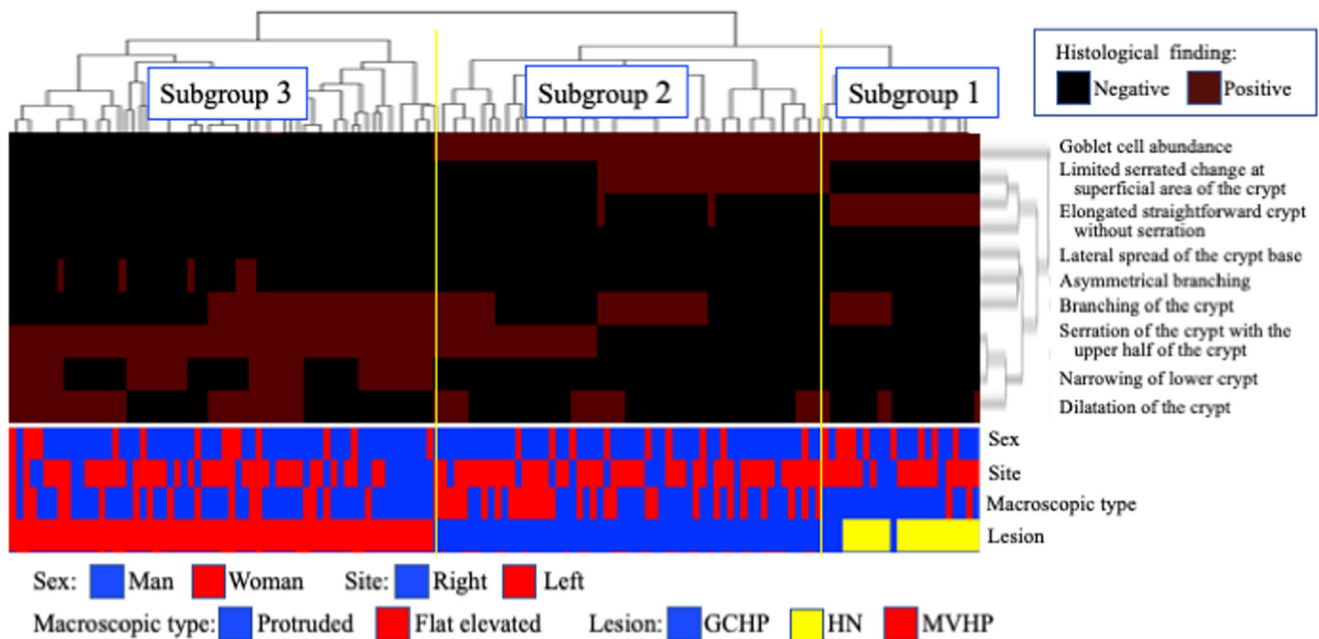
*$p < 0.01$;

#$p < 0.01$;

**$p < 0.01$.

FIGURE 2 Hierarchical cluster analysis of MVHP, GCHP, and HN hyperplastic lesions based on expression of multiple histological features. The examined hyperplastic lesion samples were classified into three subgroups. GCHP, goblet cell-rich hyperplastic polyp; HN, hyperplastic nodule; MVHP, microvesicular hyperplastic polyp

factors, the macroscopic type showed statistical differences among the three subgroups. In addition, there were significant differences in the frequencies of protruded and flat elevated types between subgroups 1 and 2 and between subgroups 1 and 3. The clinicopathological findings for each subgroup are shown in Table 4.

The frequency of HN was significantly higher in subgroup 1 than in subgroups 2 and 3; the frequency of GCHP was significantly higher in subgroup 2 than in subgroups 1 and 3; and finally, the frequency of MVHP was significantly higher in subgroup 3 than in subgroups 1 and 2. The histological findings for each subgroup are shown in Table 5.

DISCUSSION

Previous studies have suggested that hyperplastic polyps (HPs) are harmless and insignificant, and their clinical and pathological aspects were largely ignored.[1–3] However, sessile serrated lesions (SSLs), a representative type of premalignant polyp and the origin of the serrated pathway, which is closely associated with colorectal cancer (CRC) with microsatellite instability (MSI), have been segregated from HP.[1–3] In addition, MVHPs are known precursors of SSLs and traditional serrated adenoma (TSA).[1–3] Recent studies have shown that both SSLs and HPs are considered neoplastic lesions owing to their high frequencies of specific gene mutations (e.g., KRAS and BRAF).[1–3,18]

Moreover, it is becoming clear that GCHPs progress to TSA with KRAS mutations, forming a premalignant lesion that may develop to CRC with microsatellite stability.[18,19] According to these findings, HPs may not be trivial lesions in terms of molecular pathology. However, pathologists may not recognize GCHPs as having a neoplastic nature because they exhibit little or no histological atypia.[1–3,20] Among Japanese pathologists, HNs, which resemble GCHPs histologically, have been used in routine histological diagnosis. If HNs do not have any specific gene mutations, then they may be non-neoplastic lesions that should be distinguished from GCHPs, which may be preneoplastic lesions. However, the characteristics of HNs have not been thoroughly investigated in previous studies.

Accordingly, in this study, we investigated the differences in histological features among GCHPs, MVHPs, and HNs. MVHPs are characterized by four features: "serration of the crypt with the upper half of the crypt," "branching of the crypt," "dilatation of the crypt," and "narrowing of the lower crypt"; whereas "goblet cell abundance" and "limited serrated change, only at the surface of the crypt" are the most distinctive features of GCHPs. By contrast, the best histologically significant feature shared by GCHPs and HNs is "elongated straightforward crypts without serration." In the current study, our findings suggested that "goblet cell abundance" was a common finding between GCHPs and HNs and that "admixed goblet and absorptive cells" was important for differentiating HNs from GCHPs. Thus, GCHPs predominantly consisted

TABLE 4 Differences of clinicopathological findings between subgroup in colorectal hyperplastic lesions

		Subgroup 1 (%)	Subgroup 2 (%)	Subgroup 3 (%)	*p*-value
Total		22	58	62	
Man: Woman		15: 7	47: 11	48: 14	0.470
Age (years old)	Range (mean)	35–84 (72)	29–78 (61)	31–79 (61)	N. S.
Locus	Right	5 (22.7)	12 (20.7)	23 (37.1)	0.113
	Left	17 (77.2)	46 (79.3)	39 (62.9)	
Size (mm)	Range (mean)	1–10 (5)	2–20 (5)	3–13 (6)	N. S.
Macroscopical type	Protruded type	20 (90.9)*	29 (50.0)*,**	45 (72.6)**	0.00094
	Flat elevated type	2 (9.1)*	29 (50.0)*,**	17 (27.4)**	
Lesion	HN	19 (86.4)*,#	0*	0#	2.93E−54
	GCHP	3 (13.6)*	58 (100)*,#	0#	
	MVHP	0*	0#	62 (100)*,#	

Abbreviations: GCHP, goblet cell-rich hyperplastic polyp; HN, hyperplastic nodule; MVHP, microvesicular hyperplastic polyp; N. S., not significant.
*p < 0.01;
#p < 0.01;
**p < 0.01.

TABLE 5 Differences of histological findings between subgroup in colorectal hyperplastic lesions

	Subgroup 1 (%)	Subgroup 2 (%)	Subgroup 3 (%)	*p*-value
Total	22	58	62	
Goblet cell abundance	22 (100)[*]	58 (100)[#]	0[*,#]	3.25E−42
Limited serrated change at superficial area of the crypt	0[*]	33 (56.9)[*,#]	0[#]	1.66E−16
Serration of the crypt with the upper half of the crypt	0[*,#]	25 (43.1)[#,♭]	62 (100)[*,♭]	3.19E−24
Branching of the crypt	8 (36.4)	23 (39.6)	33 (53.2)	0.2202
Dilatation of the crypt	4 (18.2)[**]	14 (24.1)[##]	31 (50.0)[**,##]	0.0026
Lateral spread of the crypt base (such as boot- shaped or anchor-shaped crypts)	0	0	0	N. S.
Asymmetrical branching	0	0	6 (9.7)	0.0111
Narrowing of lower crypt	0[#]	0 [#]	36 (58.1)[*,#]	6.48E−17
Elongated straightforward crypt without serration	22 (100)[*,#]	2 (3.4)[*]	0[#]	4.14E−24

Abbreviation: N. S., not significant.

[*]$p < 0.01$;
[#]$p < 0.01$;
[♭]$p < 0.01$;
[**]$p < 0.05$;
[##]$p < 0.05$.

of goblet cells. Therefore, we suggest that HNs can best be differentiated from GCHPs in terms of the histological finding "elongated straightforward crypts without serration." Additionally, finding "admixed goblet and absorptive cells" may help to differentiate GCHPs from HNs histologically.

In this study, we demonstrated that the distribution of proliferative (Ki67-positive) cells contributed to distinct morphological changes in GCHPs, MVHPs, and HNs. Previous studies have shown that the distribution of Ki67-positive cells differs between HPs and SSLs, with a higher Ki67-positive rate and asymmetrical distribution in sessile serrated adenoma/polyps.[14,21] However, such differences were not confirmed in our study. Therefore, the symmetrical distribution of Ki67-positive cells was considered a distinctive feature in HPs, including GCHPs, MVHPs, and HNs. In the current study, although HPs expanded from the lower to the middle portion of the crypt, HNs were confined to the lower portion. This finding may be helpful to differentiate HNs from GCHPs. In addition, this finding was also confirmed by cluster analysis. According to this finding, the lower type was assigned to subgroup 1, which characterized HNs. We suggest that the distribution of Ki67-positive cells within the crypt may contribute to the differentiation of HNs from HPs.

Identification of differences in the expression of Annexin A10 among the hyperplastic lesions examined in this study may be an important point for elucidating the details of the pathogenesis of HNs.[22] Previous studies have shown that Annexin A10 expression characterizes sessile lesions, suggesting that Annexin A10 expression

may help to differentiate sessile lesions from other lesions.[22] In this regard, we attempted to investigate the expression of Annexin A10 in the hyperplastic lesions examined in this study. However, the current findings suggested that absence or low expression of Annexin A10 was common among the three types of hyperplastic lesions, including MVHPs, GCHPs, and HNs.

In the current study, although *BRAF* mutations characterized MVHPs, *KRAS* mutations were closely associated with GCHPs. The presence/absence of *BRAF* mutations may be a key molecular feature for differentiating MVHPs from GCHPs.[1–3] If a pathologist has difficulty in their differential diagnosis, genetic testing for *BRAF* mutations may help.[1–3] Next, *KRAS* mutations may be an excellent marker for differentiating GCHPs from HNs, given that this mutation showed a high frequency in GCHPs compared with that in HNs. This finding also suggested that GCHPs may have a neoplastic nature, whereas HNs are thought to be non-neoplastic. Despite their histological resemblance, we suggest that GCHPs should be differentiated from HNs. In our experience, we have not encountered cancer derived from HNs, and the malignant potential of HNs is very low. Despite this, it is still necessary to identify HNs in routine histological diagnosis because HPs (including MVHPs and GCHPs, which are well recognized as common lesions) rarely progress into CRC. Because MVHPs and GCHPs are precursors of SSLs and TSA,[23,24] we suggest that categorization of HNs is necessary in gastrointestinal pathology as a counterpart of neoplastic HPs.

In conclusion, in this study, we examined clinicopathological and molecular findings in GCHPs, MVHPs,

and HNs. The three lesions were different from one another in terms of pathological and molecular findings. HNs, which may be somewhat benign lesions both pathologically and clinically, may be important lesions to be distinguished from neoplastic GCHP lesions and precursors owing to frequent *KRAS* mutations. In addition, these findings were supported by the results of hierarchical cluster analysis using nine histological features that were closely associated with serrated lesions; such cluster analysis could be used to avoid obtaining arbitrary results. Therefore, our current findings may provide useful information to differentiate GCHPs from HNs in terms of histological and molecular findings.

ACKNOWLEDGMENTS

CONFLICT OF INTERESTS

The authors declare that there are no conflict of interests.

ETHICS STATEMENT

Informed consent was obtained from each patient according to institutional guidelines, and the research protocols were approved by the ethics committee of Iwate Medical University Hospital (reference number: MH2020-145). We guarantee that (a) the work is original; (b) the work has not been and will not be published in whole, or in part, in any other journal; and (c) all of the authors have agreed to the contents of the manuscript in its submitted form.

AUTHOR CONTRIBUTIONS

Noriyuki Uesugi, who is first author and performed all data collection and statistical analyses. Yoichi Ajioka and Tomio Arai supported the histological diagnosis. Yoshihito Tanaka performed the collection of the samples and immunohistochemical and molecular tests. Tamotsu Sugai who is the corresponding author, contributed to the preparation of the manuscript, including all aspects of the data collection and analysis.

DATA AVAILABILITY STATEMENT

The data that support the findings of our study are available from the corresponding author upon reasonable request.

REFERENCES

1. Jass JR, Whitehall VL, Young J, Leggett BA. Emerging concepts in colorectal neoplasia. Gastroenterology. 2002;123:862–76.
2. Hamilton SR, Sekine S. Conventional colorectal adenoma. WHO classification of tumours of the digestive system. Lyon: International Agency for Research on Cancer; 2019. p. 170–3
3. Leggett B, Whitehall V. Role of the serrated pathway in colorectal cancer pathogenesis. Gastroenterology. 2010;138:2088–100.
4. Cancer Genome Atlas Network. Comprehensive molecular characterization of human colon and rectal cancer. Nature. 2012;487(7407):330–7.
5. De Palma FDE, D'Argenio V, Pol J, Kroemer G, Maiuri MC, Salvator. The molecular hallmarks of the serrated pathway in colorectal cancer. Cancers. 2019;11:1017.
6. Pai RK, Bettington M, Srivastava A, Rosty C. An update on the morphology and molecular pathology of serrated colorectal polyps and associated carcinomas. Mod Pathol. 2019;32: 1390–415.
7. Japanese Society for Cancer of the Colon and Rectum. Japanese Classification of Colorectal Carcinoma. 2nd English ed. Tokyo: Kanehara Co.; 2009. p. 30–63
8. Rex DK, Ahnen DJ, Baron JA, Batts KP, Burke CA, Burt RW, et al. Serrated lesions of the colorectum: review and recommendations from an expert panel. Am J Gastroenterol. 2012;107:1315–29; quiz 1314, 1330.
9. Bateman AC. The spectrum of serrated colorectal lesions—new entities and unanswered questions. Histopathology. 2021;78: 780–90. https://doi.org/10.1111/his.14305
10. Crockett SD, Nagtegaal ID. Terminology, molecular features, epidemiology, and management of serrated colorectal neoplasia. Gastroenterology. 2019;157:949–66.e4.
11. Kim JH, Kang GH. Evolving pathologic concepts of serrated lesions of the colorectum. J Pathol Transl Med. 2020;54: 276–89.
12. Jass JR. Hyperplastic polyps and colorectal cancer: is there a link? Clin Gastroenterol Hepatol. 2004;2:1–8.
13. Sugai T, Uesugi N, Habano W, Sugimoto R, Eizuka M, Fujita Y, et al. The clinicopathological and molecular features of sporadic gastric foveolar type neoplasia. Virchows Arch. 2020;477:835–44.
14. Hisamatsu K, Noguchi K, Tomita H, Muto A, Yamada N, Kobayashi K, et al. Distinctive crypt shape in a sessile serrated adenoma/polyp: distribution of Ki67-, p16INK4a-, WNT5A-positive cells and intraepithelial lymphocytes. Oncol Rep. 2017; 38:775–84.
15. Sugai T, Eizuka M, Takahashi Y, Fukagawa T, Habano W, Yamamoto E, et al. Molecular subtypes of colorectal cancers determined by PCR-based analysis. Cancer Sci. 2017;108:427–34.
16. Yagi K, Takahashi H, Akagi K, Matsusaka K, Seto Y, Aburatani H, et al. Intermediate methylation epigenotype and its correlation to KRAS mutation in conventional colorectal adenoma. Am J Pathol. 2012;180:616–25.
17. Kaneda A, Yagi K. Two groups of DNA methylation markers to classify colorectal cancer into three epigenotypes. Cancer Sci. 2011;102:18–24.
18. Janjua HG, Høgdall E, Linnemann D. Hyperplastic polyps of the colon and rectum - reclassification, BRAF and KRAS status in index polyps and subsequent colorectal carcinoma. APMIS. 2015;123:298–304. https://doi.org/10.1111/apm.12355
19. Kim KM, Lee EJ, Ha S, Kang SY, Jang KT, Park CK, et al. Molecular features of colorectal hyperplastic polyps and sessile serrated adenoma/polyps from Korea. Am J Surg Pathol. 2011; 35:1274–86.
20. Jaravaza DR, Rigby JM. Hyperplastic polyp or sessile serrated lesion? The contribution of serial sections to reclassification. Diagn Pathol. 2020;15:140.
21. Fujimori Y, Fujimori T, Imura J, Sugai T, Yao T, Wada R, et al. An assessment of the diagnostic criteria for sessile serrated adenoma/polyps: SSA/Ps using image processing software analysis for Ki67 immunohistochemistry. Diagn Pathol. 2012;7:59.
22. Gonzalo DH, Lai KK, Shadrach B, Goldblum JR, Bennett AE, Downs-Kelly E, et al. Gene expression profiling of serrated polyps identifies annexin A10 as a marker of a sessile serrated adenoma/polyp. J Pathol. 2013;230:420–9.

23. Hashimoto T, Tanaka Y, Ogawa R, Mori T, Yoshida H, Taniguchi H, et al. Superficially serrated adenoma: a proposal for a novel subtype of colorectal serrated lesion. Mod Pathol. 2018;31:1588–98.

24. Tanaka Y, Eizuka M, Uesugi N, Kawasaki K, Yamano H, Suzuki H, et al. Traditional serrated adenoma has two distinct genetic pathways for molecular tumorigenesis with potential neoplastic progression. J Gastroenterol. 2020;55:846–57.

SUPPORTING INFORMATION

Additional supporting information may be found in the online version of the article at the publisher's website.